Journal of
ALLOYS
AND COMPOUNDS

ELSEVIER

Journal of Alloys and Compounds 223 (1995) 1–5

Electrochemical properties of $TiMn_2$-type alloys ball-milled with nickel powder

Ming Au [a], F. Pourarian [a], S. Simizu [a], S.G. Sankar [a], Lian Zhang [b]

[a] *Carnegie-Mellon Research Institute, Carnegie-Mellon University, Advanced Materials Corporation, Pittsburgh, PA 15213, USA*

[b] *Technology Laboratory, Eveready Battery Company, West Lake, OH 44154, USA*

Received 13 May 1994; in final form 29 August 1994

Abstract

$TiMn_2$-type alloys have a high hydrogen storage capacity in reaction with the hydrogen gas, but it is difficult to charge/discharge them electrochemically as negative electrode materials. In this work, we have found that by ball-milling the alloy powder with a small amount of Ni powder, their electrochemical activity can be stimulated. These ball-milled $TiMn_2$-type alloys in combination with nickel exhibit considerable discharge capacity. SEM and X-ray diffraction analyses indicated that the element nickel was distributed homogeneously on the surface of the amorphous alloy particles. The active nickel clusters presumably catalyze the electrochemical reactions in the negative electrode. The nickel spread on the surface of matrix alloy also increases corrosion resistance of the ball-milled alloys.

Keywords: Ball-milling; Electrochemical properties; Nickel

1. Introduction

Previously, we reported that certain $TiMn_2$-type alloys exhibit a high hydrogen storage capacity in the reaction with gas-phase hydrogen [1]. This work indicates that the alloy $Ti_{0.9}Zr_{0.3}Mn_{1.3}Cu_{0.05}Mo_{0.05}V_{0.2}Cr_{0.2}$ has a theoretical electrochemical energy density of 540 mA h g^{-1}. Because $TiMn_2$-type alloys are less expensive than $LaNi_5$ or $ZrNi_2$-type alloys, they are attractive candidates for negative electrode materials for rechargeable batteries. Yayama et al. [2] reported that the sintered $TiMn_{1.75}$ alloy demonstrated a discharge capacity of 32.8 mA h g^{-1} in an electrochemical cell. He also pointed out that the hydrogen absorption increases with decrease of Mn content.

In this study, several $TiMn_2$-type alloys have been studied as negative electrode materials in a beaker cell. A ball-milling technique to affect surface alloying [3] has been introduced to modify their electrochemical behavior. The effects of milling time on the electrochemical capacity, and of the ratio of nickel powder to alloy in the mixture on the electrochemical capacity, were investigated.

In order to understand the mechanism of the electrochemical behavior in relation to the processing of the anode materials, X-ray diffraction analysis (XDA), scanning electron microscopy (SEM) and electron-dispersive X-ray analysis (EDXA) were used to examine the change of the phase composition, microstructure and elemental distribution of alloys.

2. Experimental details

$TiMn_2$-type alloys were prepared from component elements with 99.9% purity by induction-melting under argon atmosphere. Each sample was remelted three times to ensure homogeneity. The ingots were annealed at 1273 K for 24 h. The crushed powders of the alloys were mixed and milled with 2 wt.% Ni powder (300 mesh) in a SPEX model 8000 Mixer/Mill. The weight ratio of hard steel balls to mixed powder is 1:1. The mill, which has only one speed (480 rev min^{-1}), was run 12 h for every sample preparation.

The ball-milled powder was analyzed using SEM and EDXA in a scanning electron microscope (Model Cam Scan, Princeton Gamma-Tech).

50 mg of the ball-milled (with or without 2 wt.% Ni) alloy powder (100–150 mesh) were mixed with 250 mg Ni powder (300 mesh) uniformly. The mixture was pressed to a porous pellet of 10 mm diameter and about 0.6 mm thickness on a copper holder under 20 MPa pressure to form the negative electrode.

0925-8388/95/$09.50
SSDI 0925-8388(94)01391-8

Table 1
Discharge capacity of $TiMn_2$-type alloys

Alloy	Discharge capacity (mA h g^{-1}) Cycle number				
	1	2	3	4	5
$Ti_{0.9}Zr_{0.3}Mn_{1.3}Cu_{0.05}Mo_{0.05}V_{0.2}Cr_{0.2}$	0	11	10	9	11
$Ti_{0.8}Zr_{0.3}Mn_{1.4}Mo_{0.1}V_{0.2}Cr_{0.2}$	0	7	8	8	7
$Ti_{0.8}Zr_{0.3}Mn_{1.4}Mo_{0.05}Cu_{0.05}V_{0.2}Cr_{0.2}$	0	5	4	5	5

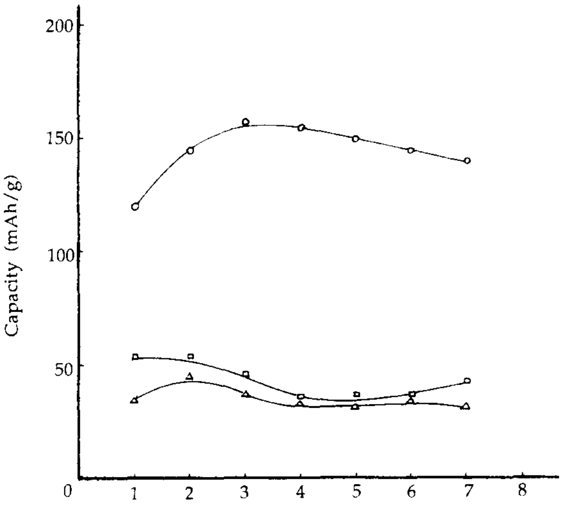

Fig. 1. Discharge capacity of ball-milled alloys (charge current, 10 mA; charge time, 3 h; discharge current, 2 mA): ○, $Ti_{0.9}Zr_{0.3}Mn_{1.3}Cu_{0.05}Mo_{0.05}V_{0.2}Cr_{0.2}$; □, $Ti_{0.8}Zr_{0.3}Mn_{1.4}Mo_{0.1}V_{0.2}Cr_{0.2}$; △, $Ti_{0.8}Zr_{0.3}Mn_{1.4}Mo_{0.05}Cu_{0.05}V_{0.2}Cr_{0.2}$.

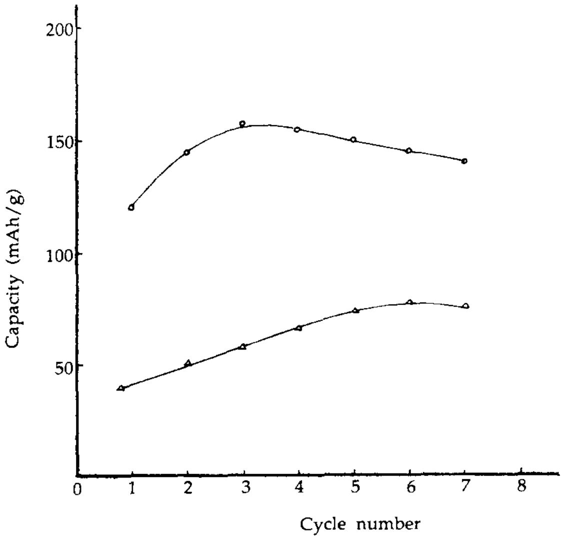

Fig. 2. Electrochemical capacity of $Ti_{0.9}Zr_{0.3}Mn_{1.3}Cu_{0.05}Mo_{0.05}V_{0.2}Cr_{0.2}$ at different discharge rates: ○, 2.5 mA; △, 10 mA.

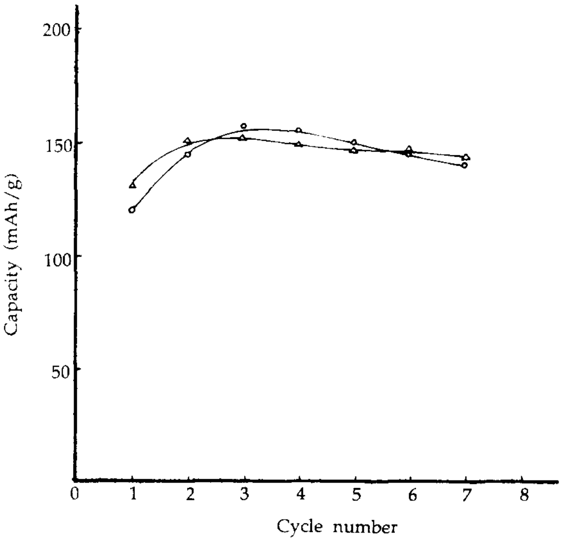

Fig. 3. Electrochemical capacity of $Ti_{0.9}Zr_{0.3}Mn_{1.3}Cu_{0.05}Mo_{0.05}V_{0.2}Cr_{0.2}$ ball-milled with different amounts of Ni powder (milling time, 12 h): ○, 2 wt.% Ni; △, 5 wt.% Ni.

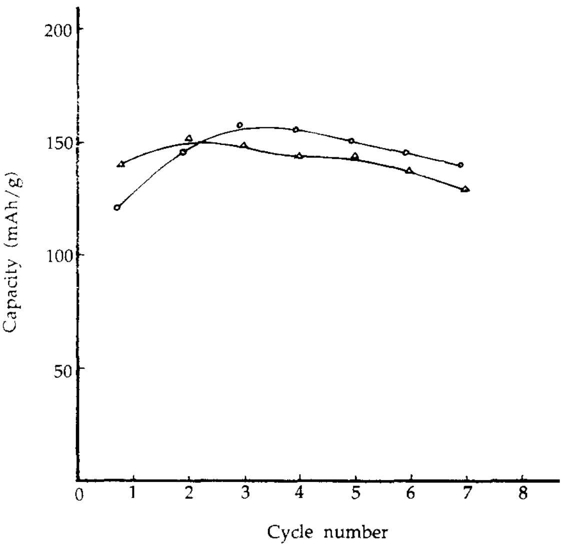

Fig. 4. Electrochemical capacity of $Ti_{0.9}Zr_{0.3}Mn_{1.3}Cu_{0.05}Mo_{0.05}V_{0.2}Cr_{0.2}$ ball-milled with 2 wt.% Ni powder for different periods: △, 12 h ball milling; ○, 24 h ball milling.

The beaker cell has three compartments, which are interconnected. The nickel hydroxide counter-electrode, an alloy negative electrode and an Hg/HgO/6 M KOH reference electrode were placed in compartments separately. The electrolyte was a 6 M KOH solution. The cell contained about 70 ml of KOH. All the measurements were carried out at room temperature. Currents of 200 mA g^{-1} for charging and 50 mA g^{-1} for discharging were employed. The end of the discharge was set to -0.600 V (cut-off voltage) with respect to the reference electrode. The constant current was supplied by a galvanostat (Model 173, Princeton Applied Research). The transformation of the crystal structure of ball-milled powder was examined with X-ray diffractometry (Model XDS5, Scintag Inc.).

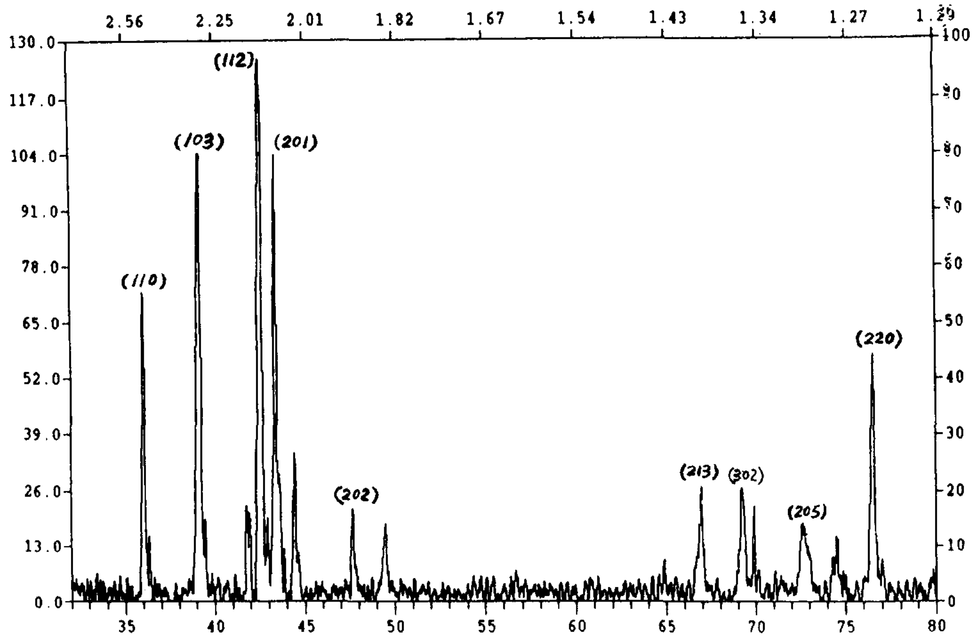

Fig. 5. X-ray diffraction pattern of $Ti_{0.9}Zr_{0.3}Mn_{1.3}Cu_{0.05}Mo_{0.05}V_{0.2}Cr_{0.2}$ alloy.

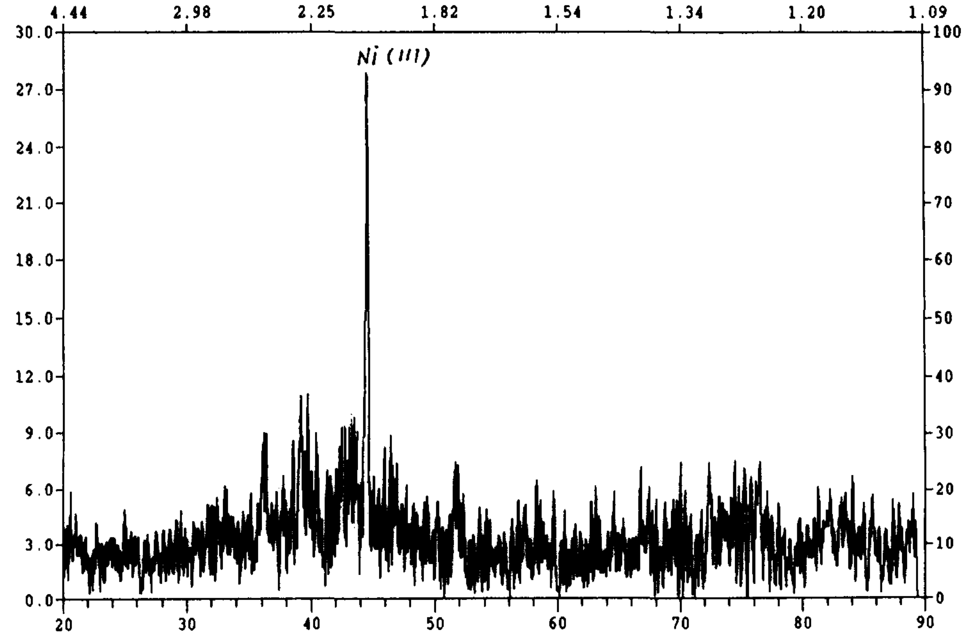

Fig. 6. X-Ray diffraction pattern of $Ti_{0.9}Zr_{0.3}Mn_{1.3}Cu_{0.05}Mo_{0.05}V_{0.2}Cr_{0.2}$ alloy ball-milled for 12 h with 2 wt.% Ni powder.

3. Results and discussion

3.1. Electrochemical measurements

3.1.1. The discharge capacity of $TiMn_2$-type alloys

Initially, the electrochemical capacity of three alloys ball-milled without Ni powder – $Ti_{0.9}Zn_{1.3}Cu_{0.05}Mo_{0.05}V_{0.2}Cr_{0.2}$, $Ti_{0.8}Zr_{0.3}Mn_{1.4}Mo_{0.1}V_{0.2}Cr_{0.2}$ and $Ti_{0.8}Zr_{0.3}Mn_{1.4}Mo_{0.05}Cu_{0.05}V_{0.2}Cr_{0.2}$ – were measured as negative electrode materials in a beaker cell. Unfortunately, only a very small amount of electrical energy was charged in these electrode materials. During the charging process, a large number of fine bubbles of hydrogen were observed to escape from the electrode surface. The potential of the negative electrode remained at a constant value. Table 1 shows the discharge capacity of these alloys. Moriwaki et al. [4] indicated that the Laves-phase alloys do not have any discharge capacity if they do not contain nickel. It is believed that the transition elements Ni, Co and Pd function as catalysts in the absorption and desorption processes of hydrogen storage alloys. This catalytic effect is expected to occur only on the surface. Therefore, a ball-milling with catalytic elements was employed as a surface

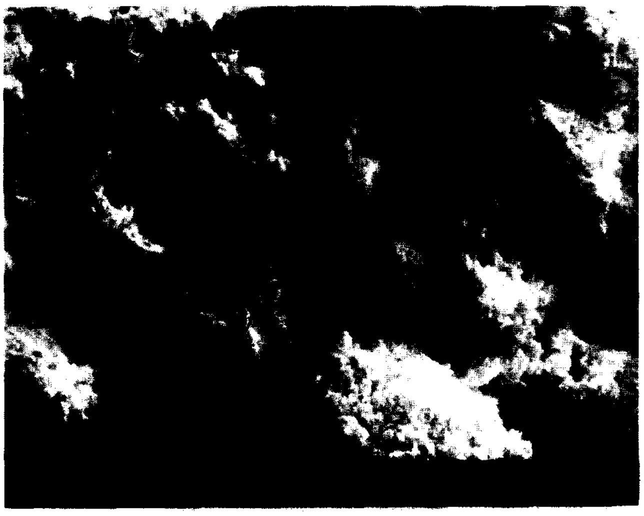

Fig. 7. SEM image of $Ti_{0.9}Zr_{0.3}Mn_{1.3}Cu_{0.05}Mo_{0.05}V_{0.2}Cr_{0.2}$ alloy powder ball-milled with 2 wt.% Ni powder for 12 h.

alloying method. So the element nickel is used to activate the surface of alloy particles and to improve the electrochemical performance of the $TiMn_2$-type alloys.

3.1.2. Discharge capacity of ball-milled $TiMn_2$-type alloys

When elemental nickel was added to the alloys in this fashion, the discharge capacity was improved dramatically owing to Ni clusters on the surface, as shown as Fig. 1. The alloy $Ti_{0.9}Zr_{0.3}Mn_{0.3}Cu_{0.05}Mo_{0.05}V_{0.2}Cr_{0.2}$ has the largest discharge capacity of 157 mA h g^{-1}. However, as shown in Fig. 2, its high-rate discharge capacity is not so satisfactory. This can be attributed to the innate slow hydriding–dehydriding kinetics, which is generally seen for the Laves-phase alloys.

Increase in the percentage of nickel powder in the ball milling mixture and longer milling time did not increase the discharge capacity (see Figs. 3 and 4).

It is notable that the amount of electrochemically desorbed hydrogen is less than that in the gas phase. This difference means that electrochemical capacity is not determined only by the hydrogen storage capacity of alloys, but also by surface chemical states, electrode potentials and electrochemical activities of alloys.

3.2. X-Ray diffraction analysis

$TiMn_2$-type alloys have the $MgZn_2$-type hexagonal crystal structure. For example, the alloy $Ti_{0.9}Zr_{0.3}Mn_{1.3}Cu_{0.05}Mo_{0.05}V_{0.2}Cr_{0.2}$ is a γ-Mn_xTi-type compound ($x = 1$–2). Its lattice parameters were found from the X-ray diffraction pattern shown in Fig. 5 to be $a = 4.982$ Å, $c = 8.155$ Å. After 12 h of ball-milling

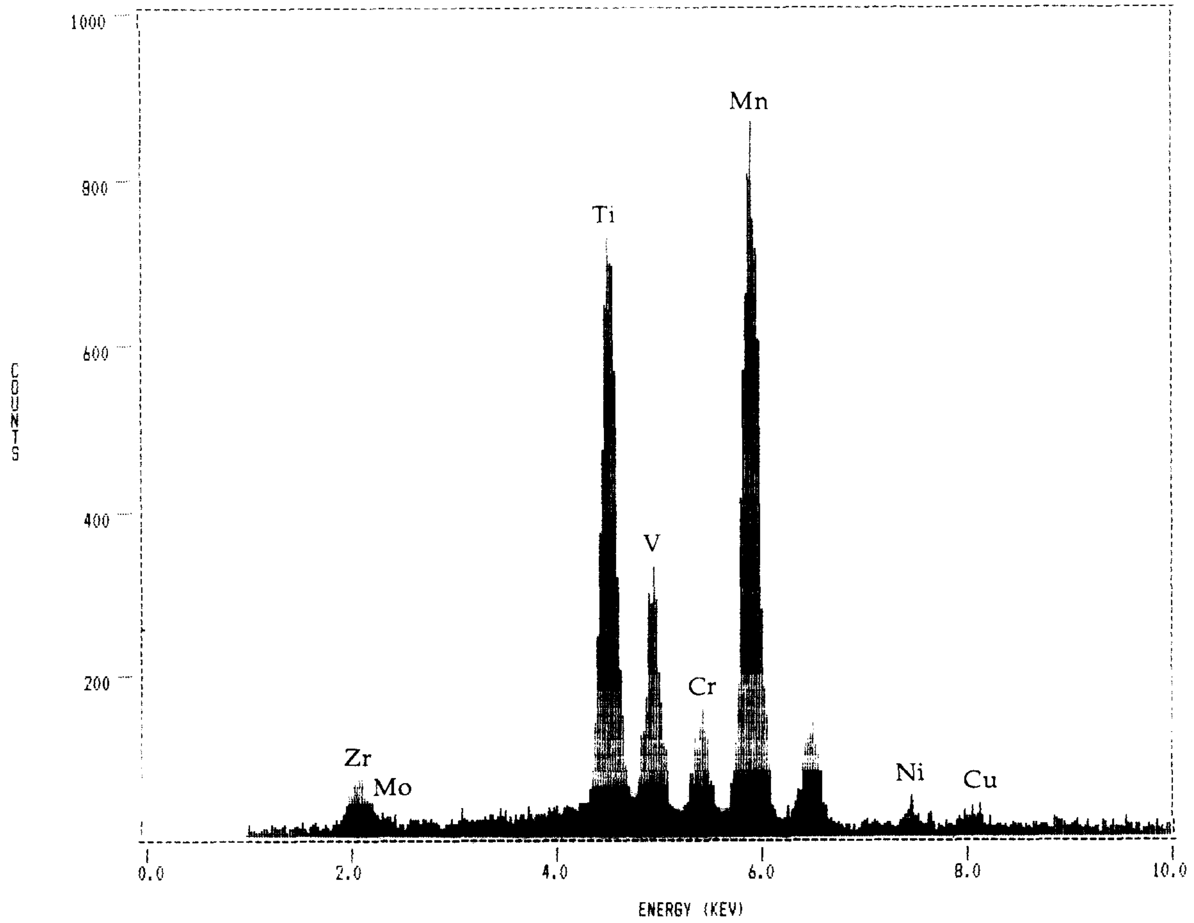

Fig. 8. EDXA spectrum of particle A in Fig. 7.

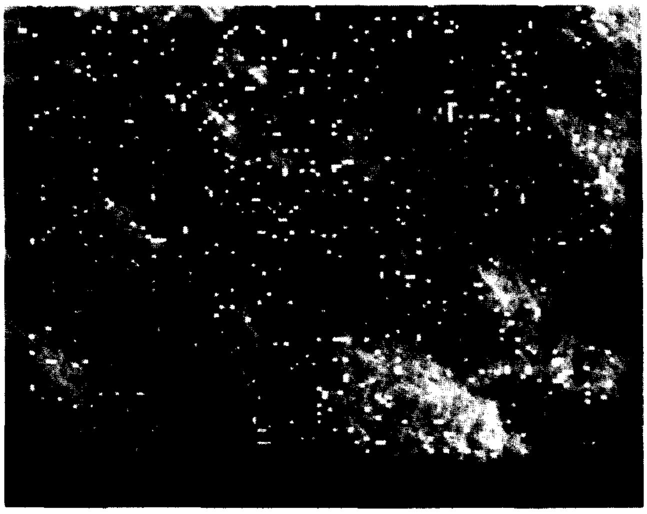

Fig. 9. SEM and EDXA scanning image of the same area as in Fig. 7. The bright spots represent qualitatively the distribution of Ni element.

with 2 wt.% Ni powder, the characteristic peaks of the γ-Mn_xTi phase disappeared. Fig. 6 shows the X-ray diffraction pattern of $Ti_{0.9}Zr_{0.3}Mn_{1.3}Cu_{0.05}Mo_{0.05}V_{0.2}Cr_{0.2}$ ball-milled with 2 wt.% Ni powder. The bulging and protruding background line indicates that the material is mainly transformed into amorphous state. A small diffraction peak attributable to the Ni (111 line) exists, although its position is shifted and its intensity reduced. This suggests that the elemental nickel partially remains in its crystal state, as a fine precipitate deposited on the surface of alloy particles. On the other hand, it is expected that chemical bonding between Ni and the matrix alloy may occur to some degree. When the Ni particles collide with alloy particles by the action of steel balls at high speed, the high kinetic energy causes cold-welding or "surface alloying" at the points of impact [5].

Another advantage of the ball-milling process is that the fresh active surface of the compound with high stress makes the surface electrochemical reaction on the electrode easier. All these may improve catalytic functioning and corrosion resistance [6].

3.3. Scanning electron microscope analysis

Fig. 7 shows the SEM morphology of $Ti_{0.9}Zr_{0.3}Mn_{1.3}Cu_{0.05}Mo_{0.05}V_{0.2}Cr_{0.2}$ powder ball-milled with 2 wt.% Ni powder. The EDXA indicated that the chemical compositions of different particles are identical. Typically, the composition of particle A (see Fig. 7) is shown in Fig. 8. The EDXA peaks of Ni were found in every particle with the same intensity, as seen in Fig. 9. In fact, no isolated pure Ni particles were found, which indicates that the Ni was distributed homogeneously on the surface of particles and combined partially with the matrix. At this partial binding state, Ni not only plays a catalyst role in the electrode reaction, but also raises the electrode potential and enhances corrosion resistance of the electrode.

4. Conclusion

$TiMn_2$-type alloys alone cannot be charged as negative electrode in a electrochemical cell. However, when modified by ball-milling with small amount of nickel powder, they exhibited a considerable charge–discharge capacity. After 12 h ball-milling with 2 wt.% Ni powder, the alloy $Ti_{0.9}Zr_{0.3}Mn_{1.3}Cu_{0.05}Mo_{0.05}V_{0.2}Cr_{0.2}$ showed 160 mA h g^{-1} discharge capacity. SEM and X-ray diffraction analysis indicated that the elemental nickel is distributed on the surface of ball-milled alloy particles homogeneously. These active Ni clusters evidently catalyze the electrode reaction in charging–discharging process. The ball-milling process transforms the material to an amorphous state. Increasing the Ni-to-alloy ratio beyond 2 wt.% in the ball-milling mixture or prolonging the milling time did not have significant effects on the discharge capacity.

Acknowledgment

The authors wish to thank the Eveready Battery Company for supporting this research.

Reference

[1] Ming Au, F. Pourarian, S.G. Sankar, W.E. Wallace and Lian Zhang, $TiMn_2$ type alloys with high hydrogen storage capacity, *Mater. Sci. Eng. B*, accepted for publication.
[2] H. Yayama, O. Ichinomiya and K. Hirakama, *J. Appl. Phys., 22(10)* (1983) L621.
[3] J.H. Harris, S. Heights, M.A. Tyenhover and R.S. Henderson, *US Patent 4 859 413.*
[4] Y. Moriwaki, T. Gamo, H. Seri and T. Iwaki, *J. Less-Common Met., 172-174* (1991) 1211–1218.
[5] A.W. Weeber and H. Bakker, *Physica B, 153* (1988) 93–135.
[6] T. Suenobu, H. Sakaguchi and G.-Y. Adachi, *J. Alloys Comp., 190* (1993) 273–277.